Nonlinear and Linear Control Law Study of Front-Wheel Steering Dynamics

William Justin Oehlschlager.*
Virginia Polytechnical Institute and State University, Blacksburg, VA, 24060

A simple model of a front wheel steering ground vehicle was studied for control during a constant velocity turn. Two control techniques were used to control the vehicle. First, the original system dynamics were linearized and an LQR control was developed. Next, the nonlinear dynamics were studied and feedback linearization was utilized to form a linear system for which an LQR controller was developed. The different controllers were tested to see the effects of various starting states would have on it and how parameter uncertainty would affect it. The two control techniques were then compared and discussed.

I. Introduction

The study of a vehicle's steering dynamics has drawn considerable attention over the years. From simple study of front wheel steering dynamics to all-wheel steering, the subject has been one of vast importance as it plays a major role in most every person's life. One of the major concerns in vehicle steering dynamics is to ensure driver safety. Due to the numerous accidents that plague our nation's roads each day the subject of improving the control of vehicles is one of constant study[1-7].

This paper deals with the study of the dynamics of vehicles under constant velocity. With a constant velocity vehicle the main dynamical concern is cornering. During most turns velocity is not held constant therefore making cornering easier on the driver by allowing a steady turn rate. However, when a vehicle moves at a constant velocity through a turn, counter-steering is usually the only course of action to ensure the car remains in a stable turn. This paper first discusses the nonlinear dynamics of a vehicle system and then linearizes the dynamics so that a linear control law can be formulated. Next, the paper takes the nonlinear dynamics and utilizes feedback linearization, a nonlinear control technique, to study the nonlinear dynamics and formulate a nonlinear control law.

* Masters Candidate, Department of Aerospace Engineering, Virginia Polytechnic Institute and State University, Blacksburg, VA.24060

II. Mathematical Model

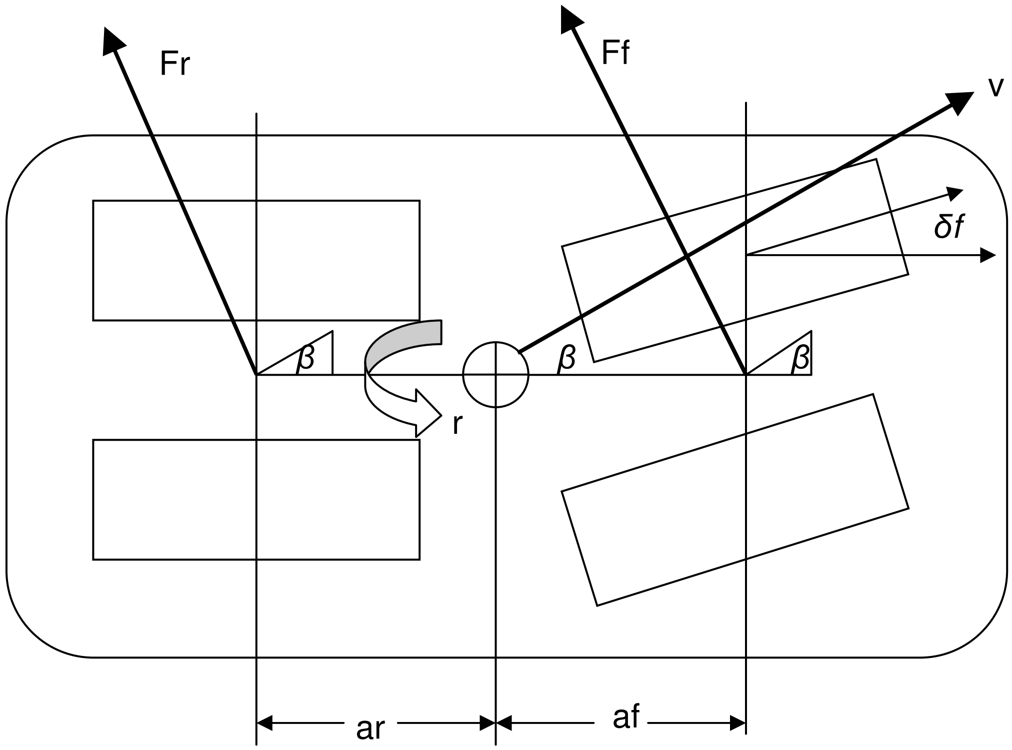

Figure 1: Vehicle Front-Wheel Steering Dynamics Model

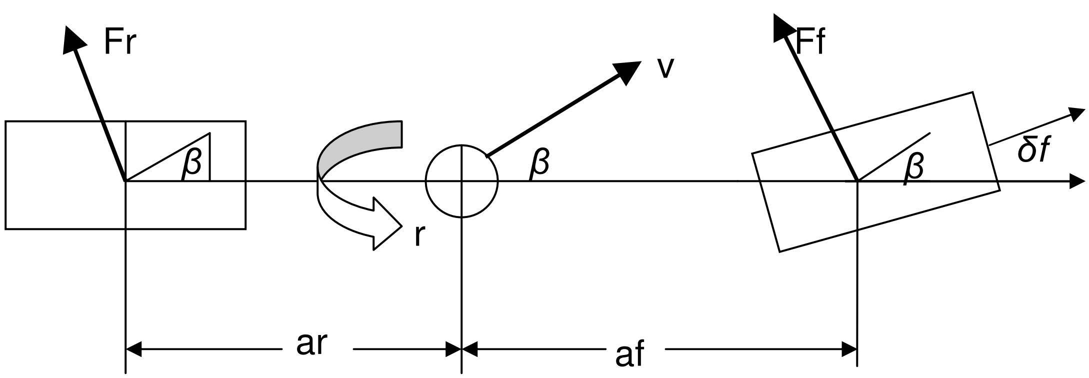

Figure 2: Half car Model for Front-Wheel Steering Dynamics

Mathematically deriving the basic equations of motion for front wheel steering dynamics with roll motion neglected is quite simple under certain assumptions. Taking the forces shown on Figure 1, one sees that the steering wheel angle δ_f and velocity v are the system inputs and yaw rate r and sideslip angle β are the system outputs. In addition, a_f represents the distance between the center of gravity (CG) and the front-wheel axes, and a_r represents the distance between the CG and the rear-wheel axes. F_f and F_r denote the combined cornering forces on the front and rear wheels respectively. In many cases, the vehicle model by lumping the two front wheels into one wheel in the center line of the car, the same procedure applies for the rear wheels and this new model is called the "half-car model" shown in Figure 2. Although simply lumping the rear and front wheels into the center line of the vehicle ignores some dynamics of the overall system, the model displays enough of the original dynamics to warrant its use. Deriving the basic equations of motion for front-wheel steering dynamics from this new model gives:

$$m(\dot{v} - v\beta r) = (F_f + F_r)\cos(\beta) - F_f \sin(\beta)\sin(\delta_f) \quad (1)$$

$$mv(\dot{\beta} + r) = F_f + F_r \quad (2)$$

$$I_z \dot{r} = (a_f F_f - a_r F_r)\cos\beta \quad (3)$$

where I_z is the yaw moment of inertia of the vehicle. In these equations F_f and F_r are formulated as functions of sideslip angles[3]

$$F_f = D_f \sin[C_f \tan^{-1}\{B_f(1-E_f)\alpha_f + E_f \tan^{-1}(B_f\alpha_f)\}] \quad (4)$$

$$F_r = D_r \sin[C_r \tan^{-1}\{B_r(1-E_r)\alpha_r + E_r \tan^{-1}(B_r\alpha_r)\}] \quad (5)$$

$$\alpha_f = \beta + \tan^{-1}(\frac{a_f}{v} r\cos\beta) - \delta_f \quad (6)$$

$$\alpha_r = \beta - \tan^{-1}(\frac{a_r}{v} r\cos\beta) \quad (7)$$

where α_f is the slip angle of the front tires, α_r is the slip angle of the rear tires, and δ_f is the front steer angle. The B_j, C_j, D_j, and E_j coefficients are given in Table 1. In this study control law development used the low friction road coefficients so that control could test for the harshest circumstances. Table 2 gives the rest of the vehicle model data as utilized in this paper. The model is taken to be a midsized passenger car.

Symbol	High Friction Road	Low Friction Road
B_f, B_r	6.7651, 9.0051	11.275, 18.631
C_f, C_r	1.3, 1.3	1.56, 1.56
D_f, D_r	-6436.8, -5430	-2574.7, -1749.7
E_f, E_r	-1.999, -1.7908	-1.999, -1.7908

Table 1: Tire Fore Coefficients

Symbol and Description	Values
M: vehicle mass	1296 kg
Iz: yaw moment	1750 kg m^2
Af	1.25 m
Ar	1.32 m
Cr0	95707 N/rad
Cf0	84243 N/rad

Table 2: Vehicle Model Variables

Taking into account the equations of motion and the fact the fact this paper describes constant velocity vehicles, the equations of motion simplify into two equations in the format

$$\begin{pmatrix} \dot{\beta} \\ \dot{r} \end{pmatrix} = \begin{pmatrix} \dfrac{F_f + F_r}{mv} - r \\ \dfrac{a_f F_f - a_r F_r}{I_z} \cos\beta \end{pmatrix} \tag{8}$$

These equations by themselves remain complicated when you include the formulations of the cornering forces on the front and rear wheels. To help simplify the matter, we will first take a look at the linear dynamics of the system and make observations about the new system before we decide upon a control law.

III. Linear Vehicle Dynamics

To obtain the linearized vehicle dynamics, the system can be linearized about an equilibrium point, but as shown in [2] there exists a linearized form of the tire force characteristics F_f and F_r. These forces are linearized as follows

$$F_f = \mu c_{f0} \alpha_f \tag{9}$$

$$F_r = \mu c_{r0} \alpha_r \tag{10}$$

$$\alpha_f = \delta_f - (\beta + \frac{a_f}{v} r) \tag{11}$$

$$\alpha_r = -(\beta - \frac{a_r}{v} r) \tag{12}$$

where c_{f0} and c_{r0} are the nominal tire cornering stiffness coefficients at μ=1, where μ is the road adhesion factor, α_f is the slip angle of the front tires, α_r is the slip angle of the rear tires, and δ_f is the front steer angle. Taking μ=0.5 for wet roads we can once again check for the worst case scenario for the control to ensure that the vehicle will be harder to control. Using this new μ, we can now define our c_r and c_f values by $c_r = \mu^* c_{r0}$ and $c_f = \mu^* c_{f0}$ respectively. In addition to these linearizations, the cos(β) term in Eq. (8) is taken to be approximately one[3]. Therefore we now have linearized state-space dynamics as follows

$$\begin{pmatrix} \dot{\beta} \\ \dot{r} \end{pmatrix} = \begin{bmatrix} \dfrac{-c_f - c_r}{mv} & -1 + \dfrac{c_r a_r - a_f c_f}{mv^2} \\ \dfrac{c_r a_r - a_f c_f}{I_z} & \dfrac{-c_r a_r^2 - a_f^2 c_f}{I_z v} \end{bmatrix} \begin{pmatrix} \beta \\ r \end{pmatrix} + \begin{bmatrix} \dfrac{c_f}{mv} \\ a_f c_f \end{bmatrix} \delta_f \tag{13}$$

Taking this system we can now alter it to add control through the steering wheel rate. This alteration leads to the linearized system

$$\begin{pmatrix} \dot{\beta} \\ \dot{r} \\ \dot{\delta}_f \end{pmatrix} = \begin{bmatrix} \dfrac{-c_f - c_r}{mv} & -1 + \dfrac{c_r a_r - a_f c_f}{mv^2} & \dfrac{c_f}{mv} \\ \dfrac{c_r a_r - a_f c_f}{I_z} & \dfrac{c_r a_r^2 - a_f^2 c_f}{I_z v} & a_f c_f \\ 0 & 0 & 0 \end{bmatrix} \begin{pmatrix} \beta \\ r \\ \delta_f \end{pmatrix} + \begin{bmatrix} 0 \\ 0 \\ 1 \end{bmatrix} u \tag{14}$$

Which is the typical linear state-space form

$$\dot{x} = Ax + Bu \tag{15}$$

With this new linear system we can now utilize regular linear control techniques to find a control law suitable to drive the system to stability.

IV. Linear Control Law Development

To develop the Linear Control Law to drive the linear system to stability, LQR[8] control is utilized. Before we start our control law development, we must first ensure that the control law will stabilize the dynamics to a pre-described equilibrium point. To do this we must first shift the equilibrium point. First we let $x_e=(\beta_e, r_e, \delta_{fe})$ be an equilibrium point so that is solves Eqs. (16) and (17).

$$0 = \frac{F_f + F_r}{mv} - r \tag{16}$$

$$0 = \frac{\cos\beta}{I_z}(a_f F_f - a_r F_r) \tag{17}$$

Now we shift the equilibrium point by using the following equations

$$\tilde{\beta} = \beta - \beta_e \tag{18}$$

$$\tilde{r} = r - r_e \tag{19}$$

$$\tilde{\delta}_f = \delta_f - \delta_{fe} \tag{20}$$

$$\begin{pmatrix} \dot{\tilde{\beta}} \\ \dot{\tilde{r}} \\ \dot{\tilde{\delta}}_f \end{pmatrix} = \begin{bmatrix} \frac{-c_f - c_r}{mv} & -1 + \frac{c_r a_r - a_f c_f}{mv^2} & \frac{c_f}{mv} \\ \frac{c_r a_r - a_f c_f}{I_z} & \frac{c_r a_r^2 - a_f^2 c_f}{I_z v} & a_f c_f \\ 0 & 0 & 0 \end{bmatrix} \begin{pmatrix} \tilde{\beta} \\ \tilde{r} \\ \tilde{\delta}_f \end{pmatrix} + \begin{bmatrix} 0 \\ 0 \\ 1 \end{bmatrix} u \tag{21}$$

So now we can stabilize the dynamics around any equilibrium we choose, including any such equilibrium that applies for a constant angle turn.

Now before we apply LQR control design we must first ensure that LQR can be applied to the system. To do that we first formulate the A matrix from Eq. (14) using the variables in Table 2 and an arbitrary velocity of 30 m/s. The A matrix is taken to be the first matrix on the right side of the equals mark as suggested by Eq.(15). Therefore the A matrix is

$$A = \begin{bmatrix} -2.3142 & -0.9910 & 1.0834 \\ 6.0084 & 0.3346 & 52651.875 \\ 0 & 0 & 0 \end{bmatrix} \tag{22}$$

This matrix provides us with stable imaginary eigenvalues, meaning that the linearized system is stable. Knowing that the system is stable the system is tested for controllability using the controllability matrix C(A,B), which shows that the system is controllable. Next, we must check for observability using the observability matrix O(A,C), but since we do not have an output for this system, C matrix, must check for observability in another fashion. The C matrix in the observability matrix is taken from a choice of a Q matrix for the LQR controller where $Q=C^TC$. Choosing Q to be 10*Identity we can easily find our C matrix and show that the system is observable. Knowing that the tests for controllabitliy and observability passed we know that we can apply LQR control to the system. Since we are using LQR we know the control is defined as

$$u = -R^{-1}B^T\overline{P}x \tag{23}$$

where $\overline{P}$ is the solution to the algebraic Riccati equation

$$0 = A^T P + PA - PBR^{-1}B^T P + Q \tag{24}$$

which minimizes the cost function

$$\lim_{T\to\infty}\int_{t0}^{T} x(\tau)^T Qx(\tau) + u(\tau)^T Ru(\tau)d\tau \tag{25}$$

With the control law decided upon we can now test the control to see how well it works with numerical simulations.

V. Numerical Simulations

Due to the altering of the linear dynamics to move the equilibrium point to any designer specified value, the final values of the system can be made to stabilize for any constant values of our states. The numerical simulations shown below have the final values of the system states equalizing to zero, this is purely for simplicity to help gain a feel for how the dynamics truly react. With this in mind several different beginning states were chosen to see how much control would be needed and how fast the control would correct the vehicle to the desired states. In these examples, the linear system was integrated to see how the control performed on the linearized system.

The first simulation uses the input states of [10;25;1.5708] with Q = [5,0,0;0,2000,0;0,0,1] and R=100. The results are shown below in Figures 3 and 4.

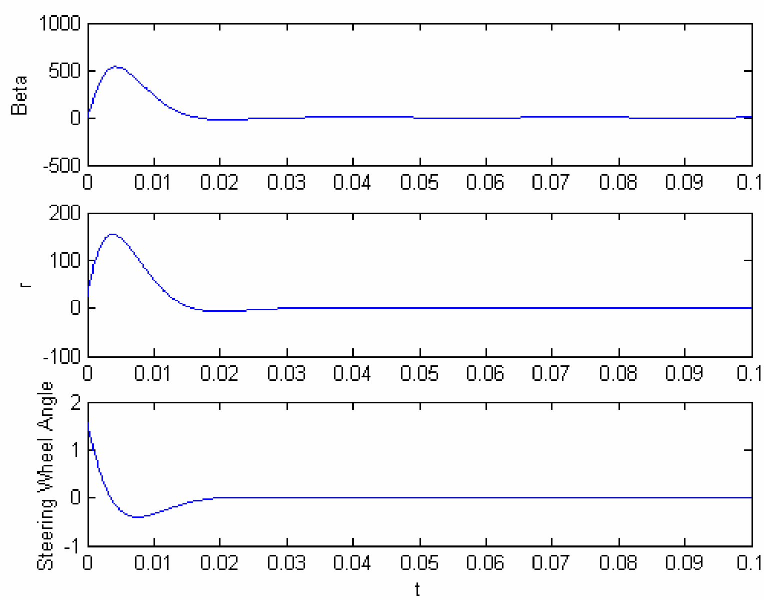

Figure 3: Various States vs. Time

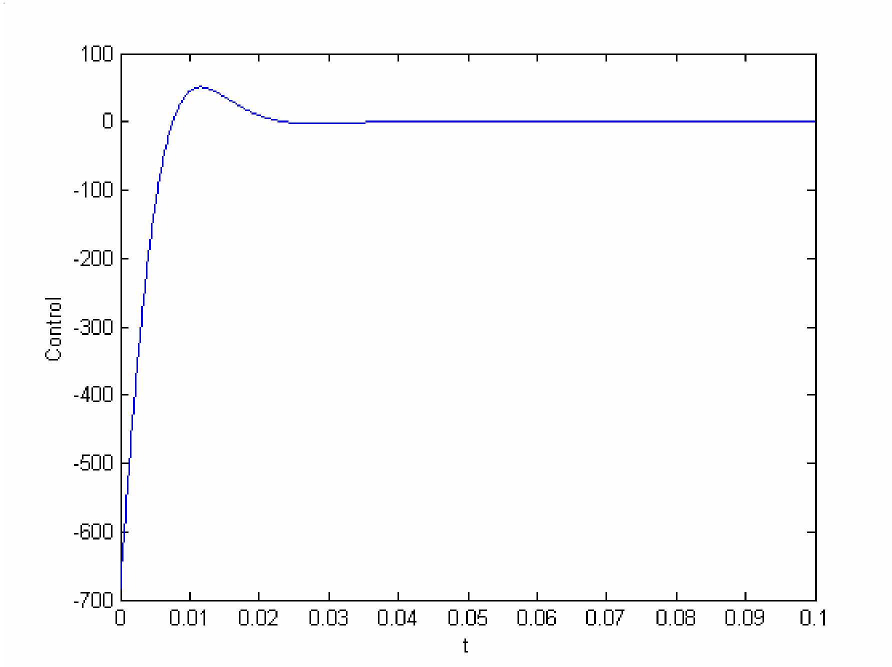

Figure 4: Control Input vs. Time

As can be seen from the above figures, the control worked to drive the system states to zero. Although, if we look at our initial states we see that our initial steering angle is 90 degrees which is impossible for most front-wheel drive vehicles. Here lies the dilemma with linearizing a nonlinear system, without properly documenting the system and setting up certain parameters that your control system can react you get impossible results as shown above. Therefore, after looking at our initial nonlinear system closer we notice a bifurcation point at δ_f = +/- 0.15 radians. Since we know that a bifurcation point exists within at these points we can conclude that our linearized system can only be valid for points within the domain of the bifurcation points. Another problem that arose from this first simulation is the massive initial control needed to help drive the system to equilibrium. Although in this numerical example the control has a massive initial input that might not be possible, the gain values on Q and R can be altered to ensure that the control stays within certain parameters and does not get saturated. However, without knowing the full limitations on what a real controller on the steering angle rate can be we can only simple assumptions can be made about how the control should be penalized to ensure the control is not saturated. The following figures show how the system stabilized with various starting states and consistent Q and R values that provide non-saturated control that was taken to be no greater that 100 N.

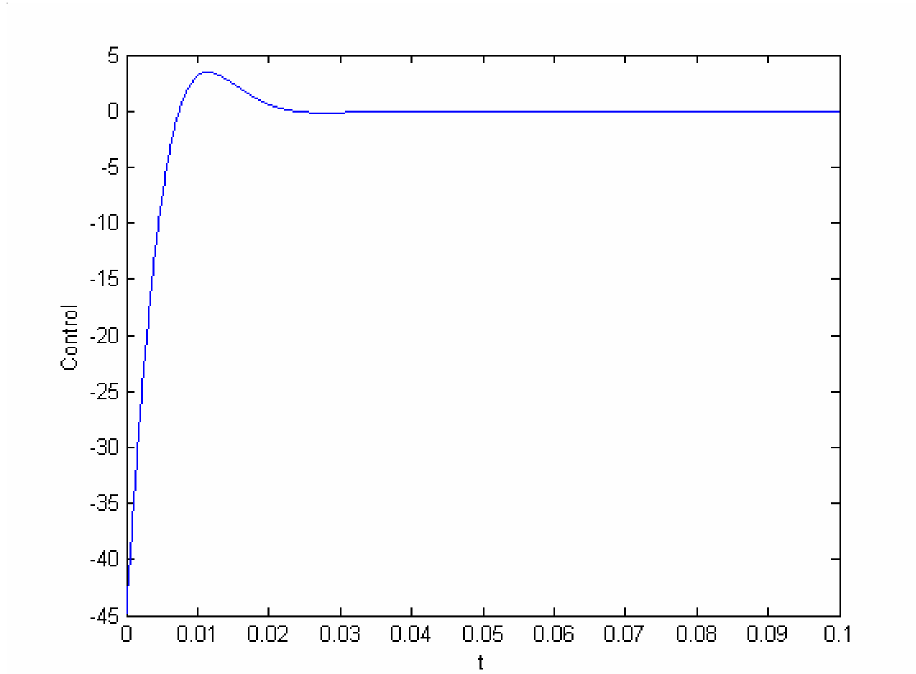

Figure 5: Control Input vs. Time Q= Q=[5,0,0;0,2000,0;0,0,1] and R=1000;

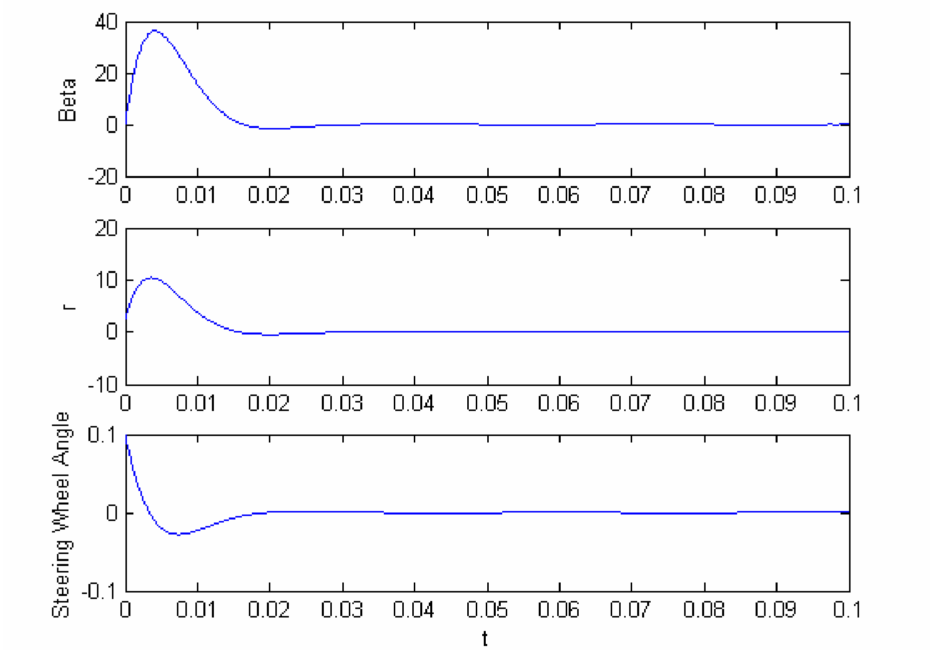

Figure 6: Various States vs. Time for X0=[0.5,2.5,0.10]

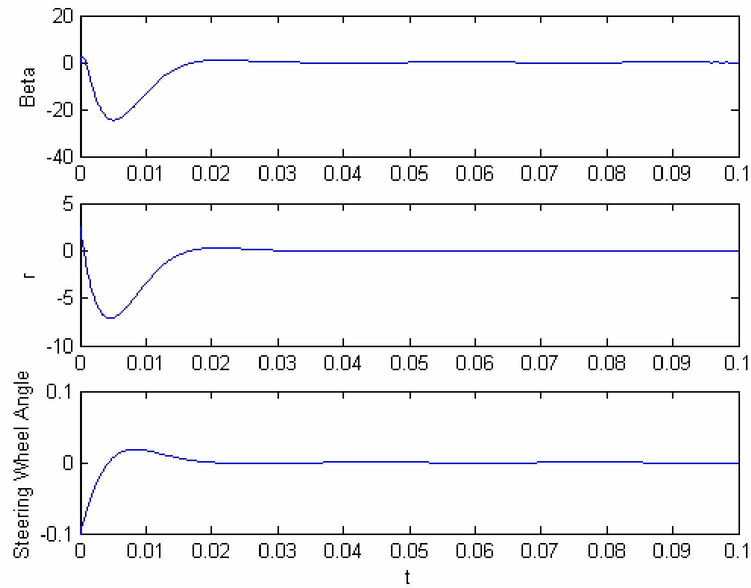

Figure 7: Various States vs. Time for X0=[-0.5,2.5,-0.10]

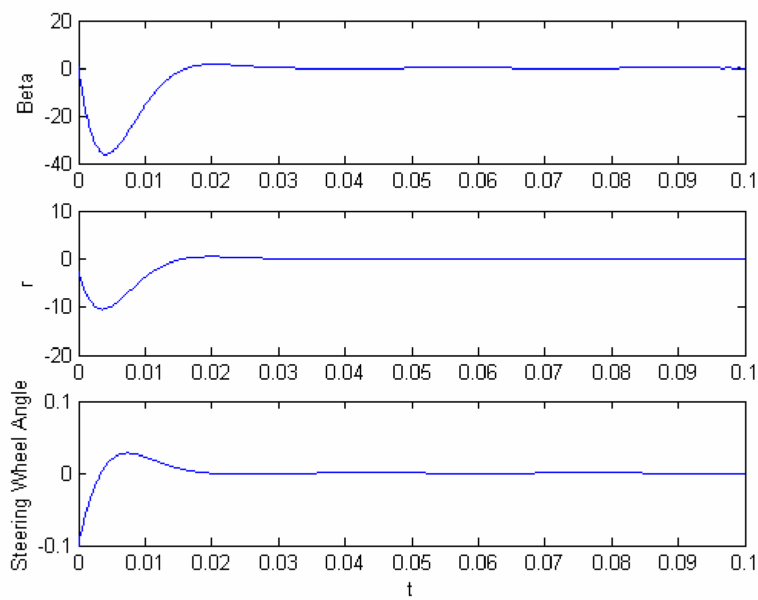

Figure 8: Various States vs. Time for X0=[0.5,-2.5,-0.10]

As can be seen in Figures 6-8 no matter how the initial states are oriented the control has no problem stabilizing the dynamics, although the dynamics do seem to trend to stabilize faster when the initial yaw rate is providing help to stabilize the system. Overall, other than a few milliseconds the beginning states do not affect the performance of the controller.

After testing the control law to see how different beginning states affected the performance, we now move on to testing for model parameter uncertainty. To test the model parameter uncertainty we will be strictly looking at the cornering stiffness variables. To vary these variables we will be altering the road adhesion values or μ on the cornering stiffness variables, while keeping the original K matrix on the control the same to see how the original control is affected. The following figures show how these changes affect the performance of the control law.

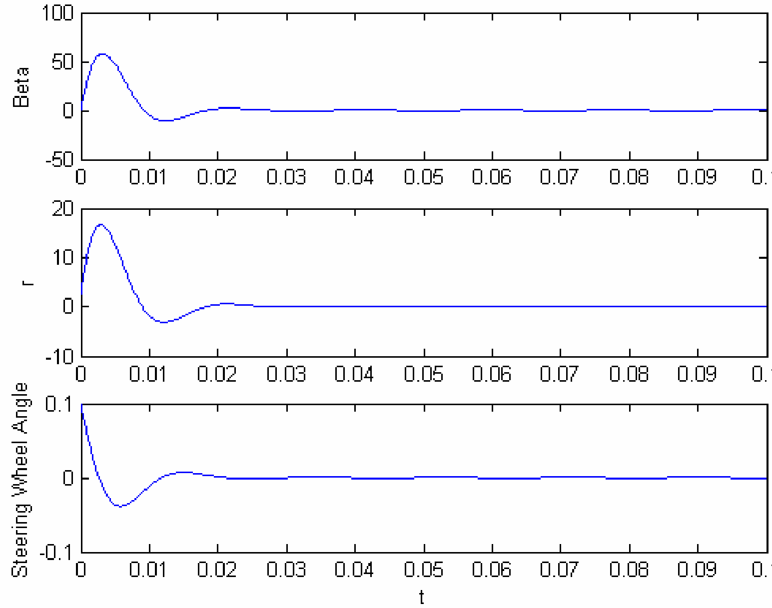

Figure 9: Various States vs. Time for μ=1 at X0=[0.5;2.5;0.10]

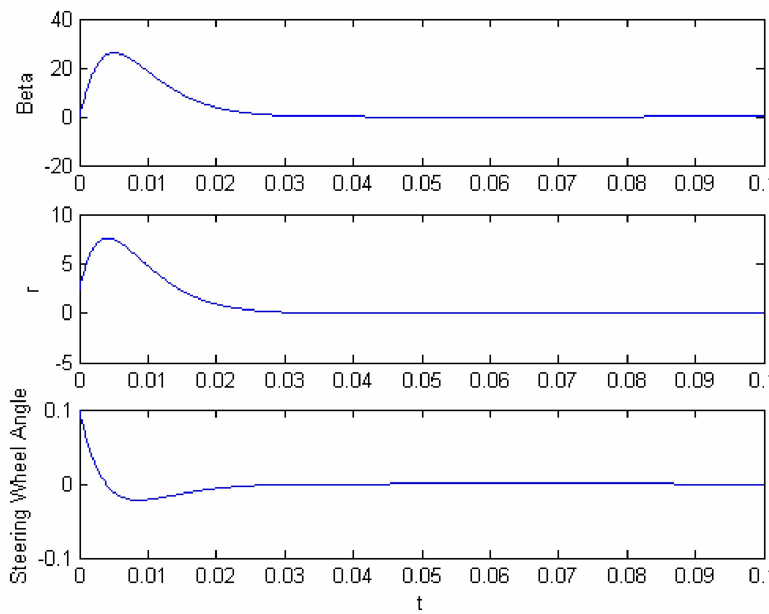

Figure 10: Various States vs. Time for μ=0.3 at X0=[0.5;2.5;0.10]

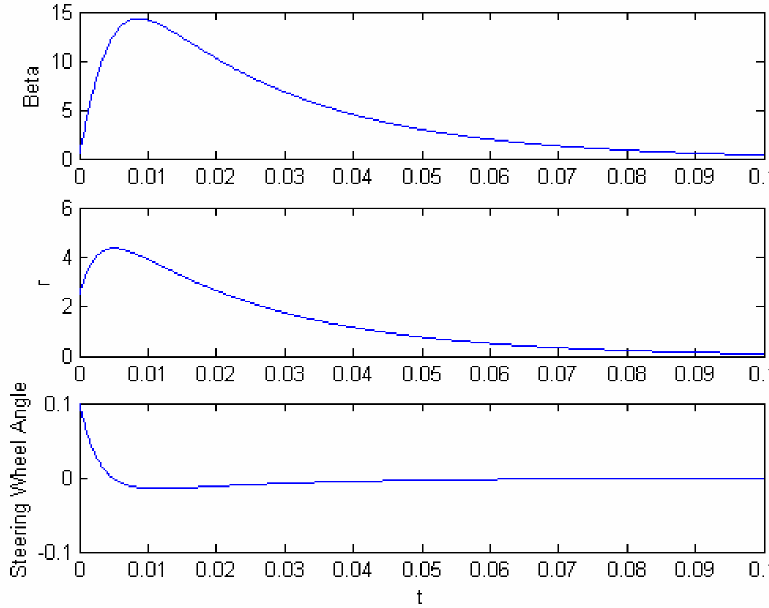

Figure 11: Various States vs. Time for μ=0.1 at X0=[0.5;2.5;0.10]

As expected with the changes in μ the system stabilized better as μ was chosen to be a larger number, signifying better road conditions. Since μ was originally chosen to apply for wet road conditions we see that the control law applies for all road conditions, even when the road is icy as evident by the conditions when μ=0.1. Now that the linear control law is complete we can focus on the nonlinear control and see how it differs.

VI. Nonlinear Control Law Development

Going back to the mathematical model for steering dynamics we can see the nonlinear dynamics from Eqs. (4) - (8). The only part missing from these equations is the dynamics for the steering control. As in the linear system, we simply add the control on the steering wheel angle and add it to the system dynamics. Once again we can develop the control for any equilibrium and simply using Eqs. (18) - (20) we can develop our new dynamics.

$$\begin{pmatrix} \dot{\tilde{\beta}} \\ \dot{\tilde{r}} \\ \dot{\tilde{\delta}}_f \end{pmatrix} = \begin{pmatrix} \dfrac{F_f(\tilde{\beta},\tilde{r},\tilde{\delta}_f) + F_r(\tilde{\beta},\tilde{r})}{mv} - (\tilde{r} + r_e) \\ \dfrac{a_f F_f(\tilde{\beta},\tilde{r},\tilde{\delta}_f) - a_r F_r(\tilde{\beta},\tilde{r})}{I_z} \cos(\tilde{\beta} + \beta_e) \\ u \end{pmatrix} \tag{26}$$

These dynamics allow us to stabilize the system about any equilibrium we choose, just like in the linear dynamics. The only problem being that nonlinear control law development is usually vastly more complicated linear control law development; therefore, this paper has chosen to use feedback linearization[9] to convert the nonlinear system to a linear system so that LQR control can once again be utilized to stabilize the system.

Before we begin our delve into feedback linearization, we must first convert the nonlinear system into the form of

$$\dot{x} = f(x) + G(x)u \tag{27}$$

which when applied to our system creates the following

$$\dot{x} = \begin{pmatrix} \dfrac{F_f(\tilde{\beta},\tilde{r},\tilde{\delta}_f) + F_r(\tilde{\beta},\tilde{r})}{mv} - (\tilde{r} + r_e) \\ \dfrac{a_f F_f(\tilde{\beta},\tilde{r},\tilde{\delta}_f) - a_r F_r(\tilde{\beta},\tilde{r})}{I_z} \cos(\tilde{\beta} + \beta_e) \\ 0 \end{pmatrix} + \begin{pmatrix} 0 \\ 0 \\ 1 \end{pmatrix} u \tag{28}$$

Now that the system is in the correct format we must first check to see if Input-State Feedback Linearization is appropriate for this problem. To check this solution we must investigate the Lie bracket condition for feedback linearization[9]. To do this we must check to see that

1. dim (span { g, ad_f g, …ad_f^{n-1} g}) = n
2. Δ(x) = span { g, ad_f g, …ad_f^{n-2} g}

Where ad_f g = [f,g] = $\dfrac{\partial g}{\partial x} f - \dfrac{\partial f}{\partial x} g$ and ad_f^2 g = [f,[f,g]]. Since our system is only 3 dimensional the first to Lie brackets are the only brackets that we need to compute. This first Lie bracket is shown below but not the second as it is too long to show here.

$$[f,g] = \begin{pmatrix} \dfrac{1}{mv}\dfrac{\partial F_f}{\partial \delta_f} \\ \dfrac{a_f \cos\beta}{Iz}\dfrac{\partial F_f}{\partial \delta_f} \\ 0 \end{pmatrix} \tag{29}$$

The brackets provide vector field along with g(x) that are linearly independent, so our first condition is satisfied. Now we must check the involutivity of Δ. The two vectors involved in Δ show us that the Lie bracket of the two vector fields is contained in the distribution of Δ so the second condition is satisfied so we can now move on with feedback linearization.

For a nonlinear system to be input-state linearizable there must be a mapping function T that converts the nonlinear system into the form in Eq. (30). This form can be manipulated using the control given in Eq. (31) to convert the dynamics into the simple linear form of the nonlinear dynamics shown in Eq. (32). From Eq. (32) we can utilize the same techniques as we used on the linear system to come up with a control law to stabilize the dynamics.

$$\dot{z} = A_c z + B_c \beta^{-1}(z)(u - \alpha(z)) \tag{30}$$

$$u(x) = \alpha(x) + \beta v \tag{31}$$

$$\dot{z} = A_c z + B_c v = \begin{pmatrix} 0 & 1 & 0 \\ 0 & 0 & 1 \\ 0 & 0 & 0 \end{pmatrix} z + \begin{pmatrix} 0 \\ 0 \\ 1 \end{pmatrix} v \tag{32}$$

We now seek a transformation of variables z=T(x) with $T_1(0)=0$ which satisfies the following requirements[9]

$$\frac{\partial T_1}{\partial x} f(x) = T_2(x) \tag{33}$$

$$\frac{\partial T_2}{\partial x} f(x) = T_3(x) \tag{34}$$

$$\frac{\partial T_3}{\partial x} f(x) = -\frac{\alpha(x)}{\beta(x)} \tag{35}$$

$$\frac{\partial T_1}{\partial x} g(x) = 0 \tag{36}$$

$$\frac{\partial T_2}{\partial x} g(x) = 0 \tag{37}$$

$$\frac{\partial T_3}{\partial x} g(x) = \frac{1}{\beta(x)} \neq 0 \tag{38}$$

Using these relationships we can find the T(x) to linearize our system. Using Eq. (36) and (37) we can see that T1 and T2 are not differentiable by δ_f. Using the knowledge that T2 is not differentiable by δ_f and Eq. (33) we come to the relationship shown in Eq. (39) which is the main equation that helps to decide upon T1(x). Using the relationship in Eq. (39) in Eq. (33) we come upon the relationship in Eq. (40). With these two relationships the relationship for T3 can now be found, which is found to be that of Eq. (41) - (43).

$$\frac{\partial T_1}{\partial \beta} = \frac{\partial T_1}{\partial r}\left(\frac{-mva_f \cos\beta}{I_z}\right) \tag{39}$$

$$T_2 = \frac{\partial T_1}{\partial r}\left(\frac{\cos\beta}{I_z}\right)(-F_r a_f - F_r a_r + rmva_f) \tag{40}$$

$$T_{3a} = \frac{\partial T_1}{\partial r}\left(\frac{F_f + F_r}{mv} - r\right)\left(\left(\frac{-\sin\beta}{I_z}(-F_r a_f - F_r a_r + rmva_f)\right) + \left(\frac{\cos\beta}{I_z}\right)\left(-\frac{\partial F_r}{\partial \beta} a_f - \frac{\partial F_r}{\partial \beta} a_r\right)\right) \tag{41}$$

$$T_{3b} = \frac{\partial T_1}{\partial r}\left(\frac{\cos\beta}{I_z}(F_f a_f - F_r a_r)\right)\left(\left(\frac{\cos\beta}{I_z}\right)\left(-\frac{\partial F_r}{\partial r} a_f - \frac{\partial F_r}{\partial r} a_r + mva_f\right)\right) \tag{42}$$

$$T_3 = T_{3a} + T_{3b} \tag{43}$$

Using these relationships, the mapping T(x) can now be formulated. First using Eq. (39) and the fact we learned before that T1 can not be differentiated by δ_f. we can formulate T1 which is shown in Eq. (44). From there we can formulate T2 which is shown in Eq. (45) and T3 which is not shown due to length.

$$T_1 = r - \frac{mva_f \sin\beta}{I_z} \tag{44}$$

$$T_2 = \left(\frac{\cos\beta}{I_z}\right)(-F_r a_f - F_r a_r + rmva_f) \tag{45}$$

Now having our mapping function and our dynamics in the form presented by Eq. (32) we can develop the control law the same as we did for the linear system above and to avoid redundancy will not be described. Instead we will move ahead to the numerical simulations and describe the findings.

VII. Numerical Simulations

The numerical simulations done on the new linear system needed vastly different Q and R matrices to stabilize the dynamics within the same time frame as above. This is due to the fact that using the same Q matrix penalized the dynamics differently in this linear system. For the first simulations shown in Figures 12 and 13 the input states are found using the original states variables of [0.5;2.5;0.10] with Q=[50000,0,0;0,2000,0;0,0,1] and R=1.

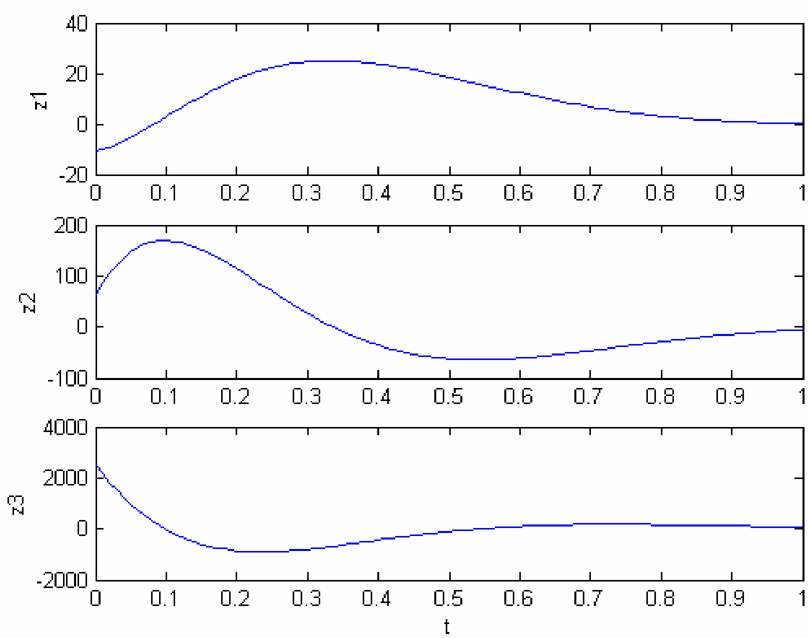

Figure 12: Various States vs. Time

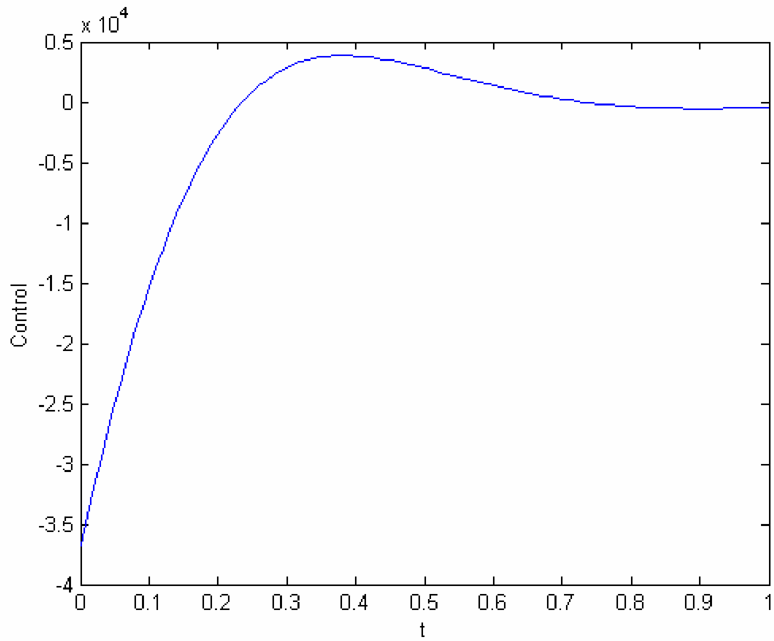

Figure 13: Control, v vs. Time

After having adjusted the Q and R matrices so that penalizes the z dynamics appropriately, we find that it suitably drives the system dynamics to zero within 1 second. Having this new Q and R decided upon we now run tests as before to see how different orientations of the state dynamics affect the control law and how fast the controller stabilizes the dynamics.

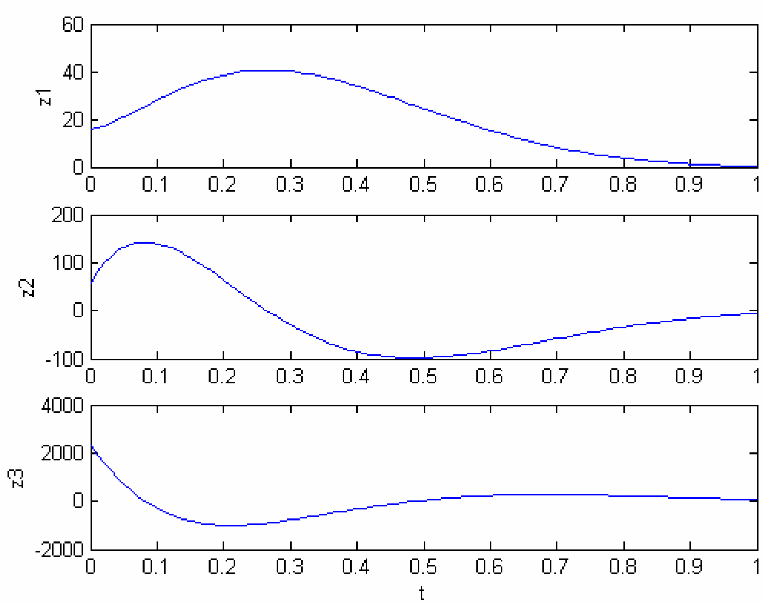

Figure 14: Various States vs. Time for X0=[-0.5,2.5,-0.10]

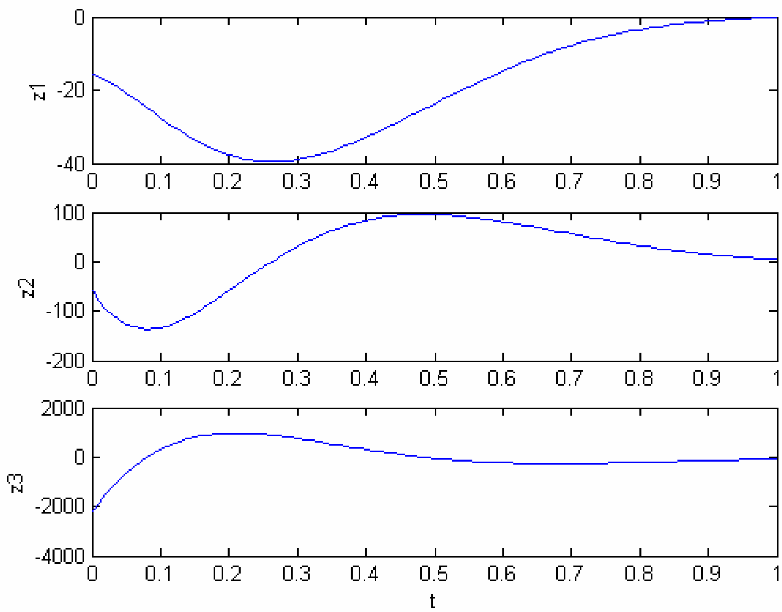

Figure 15: Various States vs. Time for X0=[0.5,-2.5,-0.10]

As can be seen in Figures 12 and 14-15 now matter where the states start or how they are oriented the control has no problem stabilizing the dynamics. Other than a few milliseconds the beginning states do not affect the performance of the controller.

After testing the control law to see how different beginning states affected the performance, we now move on to testing for model parameter uncertainty. To test the model parameter uncertainty we will be strictly looking at the tire force coefficients given in table 1. Figure 16 shows how the dynamics act when on a low friction road and Figure 17 shows how the dynamics act on a high friction road with X0=[0.5,2.5,0.10]. Once again these tests were run utilizing the same K matrix that was initially defined from the low friction road so the friction effect of the road can be seen. These Figures seem deceiving seeing how the dynamics for the higher friction road seem to make the dynamics act more unstable than for those for the low friction road for certain states and act better for other states. Although since the z parameters are not exactly the dynamics of the vehicle it does not mean much unless you try to locate where the parameter differences might be coming from exactly. Instead of trying to locate the exact parameter differences the dynamics for the first linear system are mapped into the z coordinates using the mapping functions to see the side by side comparison of how the dynamics are affected. As noticed from Figure 19, the linear system first utilized left out some major effects in the dynamics that the feedback linearization still accounts for. The main contribution to these differences comes from the fact that it was a lot easier and faster to stabilize the linear dynamics than the nonlinear dynamics, which is evident from the high gain values on the feedback linearized system. Although, as we relax the gains imposed on our linear system we see that the feedback linearized system makes a smoother transition to equilibrium as shown in Figure 20. As we look toward the total control of the system u, we can notice that for the nonlinear system much more control is needed that for the linear system as shown in figure 21. Overall, the controller worked just as expected from the linear dynamics we studied before and showed some similar results on the nonlinear system once feedback linearization was utilized. It showed that although the linear system made the control of the dynamics much easier it left out some important dynamics that show up in the nonlinear system.

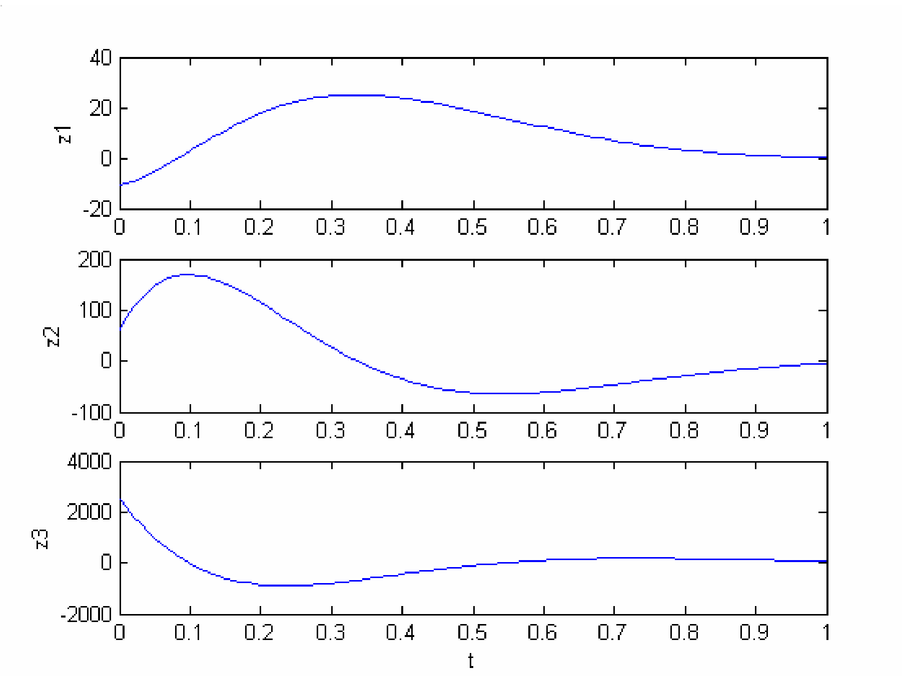

Figure 17: Various States vs. Time for Low Friction Road

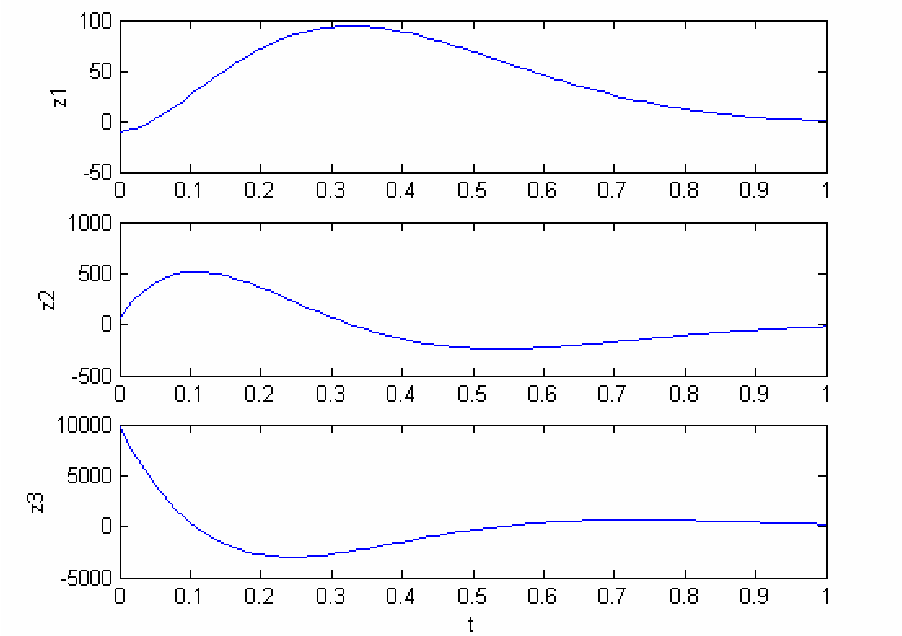

Figure 18: Various States vs. Time for High Friction Road

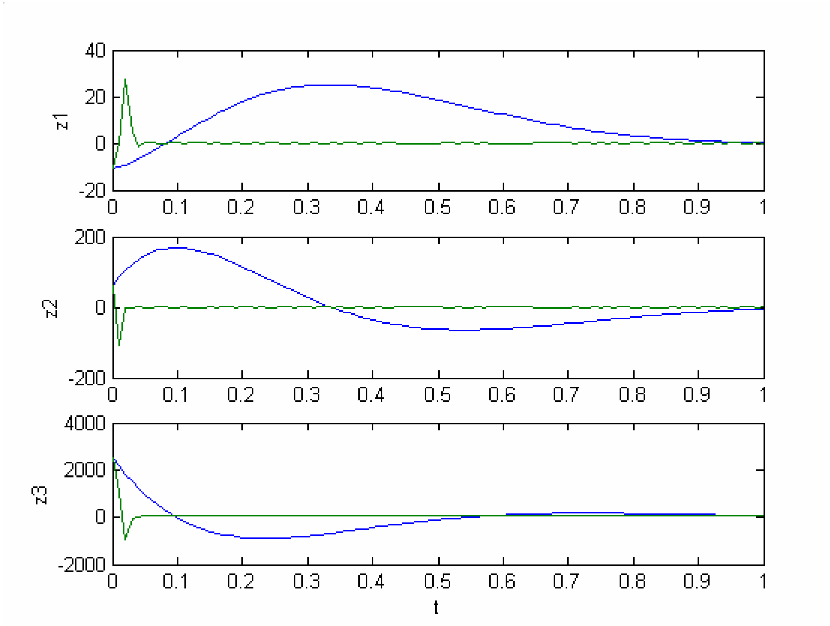

Figure 19: Various States vs. Time for Both Control Techniques
Blue: Feedback Linearizaion Green: Linear System

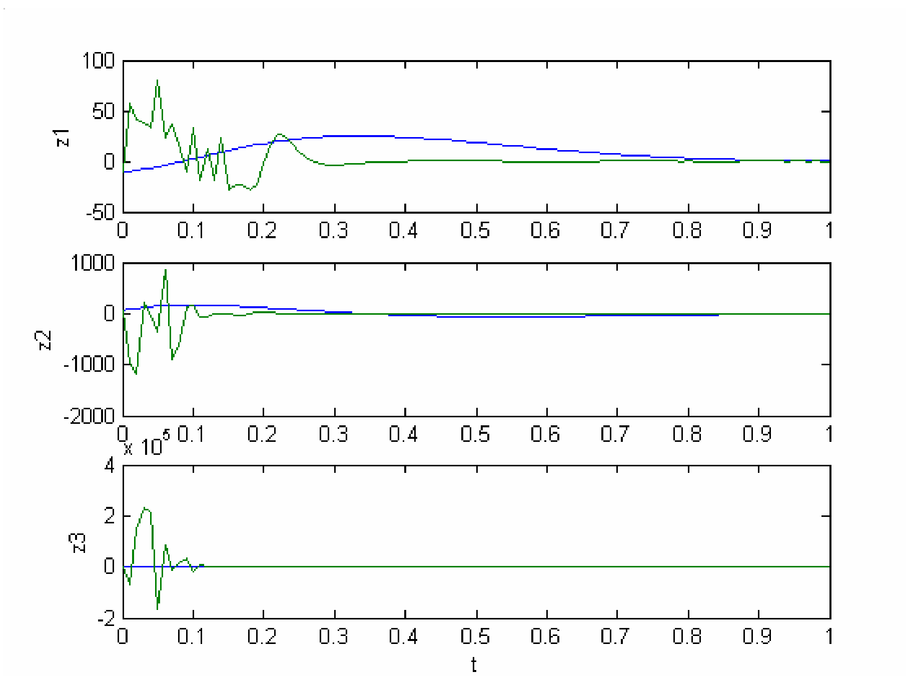

Figure 20: Various States vs. Time for Both Control Techniques

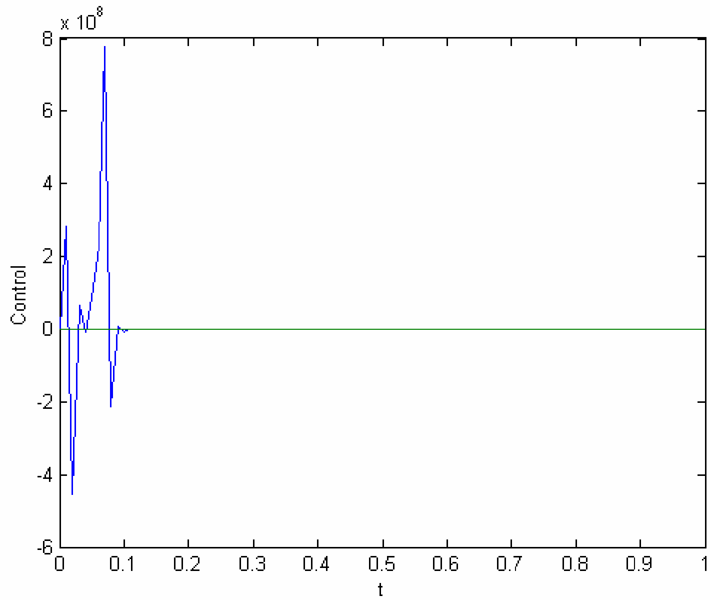

Figure 21: Control vs. Time for Both Control Techniques

VIII. Conclusion

Throughout this paper a simple model of a front wheel steering ground vehicle was studied under two very different circumstances. First, the vehicle was studied for its linearized dynamics and a control law, LQR control, was formulated to maintain equilibrium during a constant radius turn. Second, the vehicle was studied under nonlinear circumstances and nonlinear techniques were used to formulate a control law to maintain equilibrium. These techniques involved feedback linearization to form a linear system that LQR control could then be applied to. Although the two different approaches both ended up using linear control law techniques they helped to show the benefits of having linear control design instead of nonlinear in certain circumstances. Even though the nonlinear control law provided a more in depth control on the actual system a linear controller seemed to have good enough control to drive the system to equilibrium during simple maneuvers. The linear system also proved to have smaller gains and control values needed than the nonlinear system which show why in most cases linear dynamics are chosen to control vehicle dynamics. Although the feedback linearized nonlinear system proved to difficult to inverse map into original dynamic parameters to test the differences in the control law a simple mapping of the linear system into the feedback linearized system proved good enough to draw conclusions from.

This study brought about several questions involving how the system would react when velocity was not held constant. The system seemed much more complicated under these circumstances and it was found that the nonlinear system could not be input feedback linearized so the study was abandoned. The introduction of velocity playing a more important role in the dynamics means that new control techniques would have to be utilized. Although not studied in this paper it provides an interesting subject for future research.

Appendix

Programs for Simulations

Linear Main Program

```
global A B K

%Model Variables
af=1.25;
ar=1.32;
Iz=1750;
m=1296;
v=30;

%Cornering Stiffness Variables
cf=0.1*84243;
cr=0.1*95707;

%A matrix formulation
a11=(-cf-cr)/m*v;
a12=-1+((cr*ar-af*cf)/m*v^2);
a13=cf/(m*v);
a21=((cr*ar-af*cf)/Iz);
a22=((cr*ar^2-af^2*cf)/(Iz*v));
a23=af*cf;


A=[a11,a12,a13;a21,a22,a23;0,0,0];
B=[0;0;1];
Q=[5,0,0;0,2000,0;0,0,1];
R=100;

[K,S,E]=lqr(A,B,Q,R);

tspan = [0:0.0001:0.1];
y0 = [10;25;0.15];%[0.1;-2;5]
[t,y] = ode45('proj12',tspan,y0);
LineType = '-';
LineColor = 'b';

figure(1)
subplot(3,1,1)
plot(t,y(:,1))
hold on
ylabel('Beta')

subplot(3,1,2)
plot(t,y(:,2))
hold on
ylabel('r')

subplot(3,1,3)
plot(t,y(:,3))
hold on
ylabel('Steering Wheel Angle')
```

```
xlabel('t')

v=length(t);
u=zeros(v,1);
for i=1:1:v
   n=y(i,:);
   n=n';
   u(i)=-K*n;
end
figure(2)
plot(t,u)
hold on
ylabel('Control')
xlabel('t')
```

Linear Integration File

```
function xdot = proj12(t,x)

global A B K

xdot=(A-B*K)*x;
```

Nonlinear Main Program

```
global A B K

A=[0,1,0;0,0,1;0,0,0];
B=[0;0;1];
Q=[500,0,0;0,2000,0;0,0,1];
R=100;

[K,S,E]=lqr(A,B,Q,R);

%Road Surface Variables for low friction road
Bf=11.275;
Br=18.631;
Cf=1.56;
Cr=1.56;
Df=-2574.7;
Dr=-1749.7;
Ef=-1.999;
Er=-1.7908;

Bf=6.7651;
Br=9.0051;
Cf=1.3;
Cr=1.3;
Df=-6436.8;
Dr=-5430;
Ef=-1.999;
Er=-1.7908;


%Model Variables
af=1.25;
```

```
    ar=1.32;
    Iz=1750;
    m=1296;
    v=30;

    tspan = [0:0.01:5];
    beta=5;
    r=5;
    delta_f=0.15;

    T1=r-m*v*af/Iz*sin(beta);
    T2=cos(beta)/Iz*(-Dr*sin(Cr*atan(Br*(1-Er)*(beta-
atan(af/v*r*cos(beta)))+Er*atan(Br*(beta+atan(af/v*r*cos(beta))-delta_f))))*af-Dr*sin(Cr*atan(Br*(1-Er)*(beta-
atan(af/v*r*cos(beta)))+Er*atan(Br*(beta+atan(af/v*r*cos(beta))-delta_f))))*ar+r*m*v*af);
    T3=                                                    -((Df*sin(Cf*atan(Bf*(1-Ef)*(beta+atan(af/v*r*cos(beta))-
delta_f)+Ef*atan(Bf*(beta+atan(af/v*r*cos(beta))-delta_f))))+Dr*sin(Cr*atan(Br*(1-Er)*(beta-
atan(af/v*r*cos(beta)))+Er*atan(Br*(beta+atan(af/v*r*cos(beta))-delta_f)))))/m*v-r)*sin(beta)/Iz*(-
Dr*sin(Cr*atan(Br*(1-Er)*(beta-atan(af/v*r*cos(beta)))+Er*atan(Br*(beta+atan(af/v*r*cos(beta))-delta_f))))*af-
Dr*sin(Cr*atan(Br*(1-Er)*(beta-atan(af/v*r*cos(beta)))+Er*atan(Br*(beta+atan(af/v*r*cos(beta))-
delta_f))))*ar+r*m*v*af)+cos(beta)/Iz*(-af*Dr*cos(Cr*atan(Br*(1-Er)*(beta-
atan(af/v*r*cos(beta)))+Er*atan(Br*(beta+atan(af/v*r*cos(beta))-delta_f))))*Cr*(Br*(1-
Er)*(1+af/v*r*sin(beta)/(1+af^2/v^2*r^2*cos(beta)^2))+Er*Br*(1-
af/v*r*sin(beta)/(1+af^2/v^2*r^2*cos(beta)^2))/(1+Br^2*(beta+atan(af/v*r*cos(beta))-delta_f)^2))/(1+(Br*(1-
Er)*(beta-atan(af/v*r*cos(beta)))+Er*atan(Br*(beta+atan(af/v*r*cos(beta))-delta_f)))^2)-Dr*cos(Cr*atan(Br*(1-
Er)*(beta-atan(af/v*r*cos(beta)))+Er*atan(Br*(beta+atan(af/v*r*cos(beta))-delta_f))))*Cr*(Br*(1-
Er)*(1+af/v*r*sin(beta)/(1+af^2/v^2*r^2*cos(beta)^2))+Er*Br*(1-
af/v*r*sin(beta)/(1+af^2/v^2*r^2*cos(beta)^2))/(1+Br^2*(beta+atan(af/v*r*cos(beta))-delta_f)^2))/(1+(Br*(1-
Er)*(beta-atan(af/v*r*cos(beta)))+Er*atan(Br*(beta+atan(af/v*r*cos(beta))-
delta_f)))^2)*ar)+cos(beta)^2/Iz^2*(af*Df*sin(Cf*atan(Bf*(1-Ef)*(beta+atan(af/v*r*cos(beta))-
delta_f)+Ef*atan(Bf*(beta+atan(af/v*r*cos(beta))-delta_f))))-Dr*sin(Cr*atan(Br*(1-Er)*(beta-
atan(af/v*r*cos(beta)))+Er*atan(Br*(beta+atan(af/v*r*cos(beta))-delta_f))))*ar)*(-af*Dr*cos(Cr*atan(Br*(1-
Er)*(beta-atan(af/v*r*cos(beta)))+Er*atan(Br*(beta+atan(af/v*r*cos(beta))-delta_f))))*Cr*(-Br*(1-
Er)*af/v*cos(beta)/(1+af^2/v^2*r^2*cos(beta)^2)+Er*Br*af/v*cos(beta)/(1+af^2/v^2*r^2*cos(beta)^2)/(1+Br^2*(b
eta+atan(af/v*r*cos(beta))-delta_f)^2))/(1+(Br*(1-Er)*(beta-
atan(af/v*r*cos(beta)))+Er*atan(Br*(beta+atan(af/v*r*cos(beta))-delta_f)))^2)-Dr*cos(Cr*atan(Br*(1-Er)*(beta-
atan(af/v*r*cos(beta)))+Er*atan(Br*(beta+atan(af/v*r*cos(beta))-delta_f))))*Cr*(-Br*(1-
Er)*af/v*cos(beta)/(1+af^2/v^2*r^2*cos(beta)^2)+Er*Br*af/v*cos(beta)/(1+af^2/v^2*r^2*cos(beta)^2)/(1+Br^2*(b
eta+atan(af/v*r*cos(beta))-delta_f)^2))/(1+(Br*(1-Er)*(beta-
atan(af/v*r*cos(beta)))+Er*atan(Br*(beta+atan(af/v*r*cos(beta))-delta_f)))^2)*ar+m*v*af);
    z0=[T1;T2;T3];

    [t,y] = ode45('proj22',tspan,z0);
    LineType = '-';
    LineColor = 'b';

    figure(1)
    subplot(3,1,1)
    plot(t,y(:,1))
    hold on
    ylabel('z1')

    subplot(3,1,2)
    plot(t,y(:,2))
    hold on
    ylabel('z2')
```

```
subplot(3,1,3)
plot(t,y(:,3))
hold on
ylabel('z3')
xlabel('t')

v=length(t);
u=zeros(v,1);
for i=1:1:v
    n=y(i,:);
    n=n';
    u(i)=-K*n;
end
figure(2)
plot(t,u)
hold on
ylabel('Control')
xlabel('t')
```

Nonlinear Integration File

```
function zdot = proj22(t,z)

global A B K

zdot=(A-B*K)*z;
```

References

[1]Ackermann, J. Robust Car Steering by Yaw Rate Control, at 29th Conference on Decision and Control, Honolulu, Hawaii, December 1990.

[2]Guvenc, Bilin Aksun; Dunte, Tilman; Odenthal, Dirk; Guvenc, Levent. Robust Two Degree-of-Freedom Vehicle Steering Controller Design, IEEE Transactions on Control Systems Technology. Vol. 12, No. 14, July 2004.

[3]Ono, Eiichi; Hosoe, Shigeyuki; Tuan, Hoang D.; Doi, Shun;ichi. Bifurcation in Vehicle Dynamics and Robust Front Wheel Steering Control, IEEE Transactions on Control Systems Technology. Vol. 6, No. 3, May 1998.

[4]Ackerman, Jurgen; Guldner, Jurgen; Sienel, Wolfgang; Steinhauser, Reinhold; Utkin, Vadim I. Linear and Nonlinear Controller Dsign for Robust Automatic Steering, IEEE Transactions on Control Systems Technology. Vol. 3, No. 1, March 1995.

[5]Ackerman, Jurgen; Guldner, Jurgen; Utkin, Vadim I. A Sliding Mode Control Approach to Automatic Car Steering, American Control Conference, Baltimore, Maryland, June 1994.

[6]Ha, In-Joong; Tugcu, A. Kemal; Boustany, Nader M. Feedback Linearizing Control of Vehicle Longitudinal Acceleration, IEEE Transactions on Automatic Control. Vol. 34, No. 7, July 1989.

[7]Liaw, Der-Cherng; Chiang, Hsin-Han; Lee Tsu-Tian, A Bifurcation Study of Vehicle's Steering Dynamics. Deparment of Electrical and Control Engineering, National Chiao Tung University, Hsinchu, Taiwan, R.O.C. 2005.

[8]Dorato, Peter; Abdallah, Chaouki T. Linear Quadratic Control: An Introduction, Krieger Publishing Company, Malabar Florida, 2000.

[9]Khalil, Hassan K. Nonlinear Systems, Prentice Hall, Upper Saddle River, New Jersey, 2002